Sensitization of ZnO Surface Through Cyanidin Functionalization

Arrigo Calzolari

CNR-NANO Istituto Nanoscienze, Centro S3, via campi 213A I-41125 Modena, Italy; and Physics Departmet, University of North Texas, Denton TX, USA
arrigo.calzolari@nano.cnr.it

Received 3 June 2015; Accepted 13 July 2015;
Publication 17 July 2015

Abstract

By using simulations from first principles, we investigate the electronic and optical properties of the hybrid interface resulting from the functionalization of the non-polar ZnO($10\bar{1}0$) surface due to the adsorption of cyanidin dye. This system has been proposed as metal-free active element for dye sensitized solar cell applications. However, despite the intense sensitization activity, the resulting solar cells provided extremely low conversion efficiency. Our results elucidate the microscopic mechanisms that regulate the light harvesting and the photocharge injection/ricombination at the interface, and provide an explanation of the dramatically low efficiency reported by the experiments.

Keywords: photovoltaics, anthocyanidin, ZnO, DFT, DSSC.

1 Introduction

The recent possibilities of handling single molecules and inorganic materials at the nanoscale opened the way to novel classes of solar cells [1] alternative to the standards based on Si crystals. In particular, dye-sensitized solar cells (DSSCs) have been showed very high efficiency results (10–15%) [2]. Most conventional DSSCs are constituted of a $\sim 10 \mu m$ thick film of oxide nanoparticles (usually TiO_2 or ZnO), sensitized with a monolayer of molecular dyes

Journal of Self-Assembly and Molecular Electronics, Vol. 3, 1–12.
doi: 10.13052/jsame2245-4551.2015003

(e.g. N719 black dye), adsorbed on their surfaces to harvest the visible solar radiation and generate electrical current. The mesoporous film is deposited on a transparent conducting substrate (e.g. indium-tin-oxide ITO glass), which forms the anode of the device. A liquid redox electrolyte (e.g. iodine/triiodine) and a metallic cathode close the electrical circuit. In principle, the working process is simple: electrons are photo-excited within the dyes and subsequently injected into the conduction band of the oxide semiconductor. The generated electrons diffuse by hopping through the nanopaticles up to be collected in the anode electrode. Positively charged dyes are then reduced in the electrolyte that restore the initial conditions.

From the experimental point of view, great effort has been dedicated to the synthesis of several molecular dyes [3, 4] in order to maximize the optically-active surface and to enlarge the absorbed radiation range, searching for an enhancement of the light harvesting and the charge generation. Furthermore, novel architectures based on ordered arrays of oxide nanowires [5, 6] have been proposed in order to facilitate the electron migration towards the anode collector and to reduce the exciton recombination [7].

The expectation for the next generation of DSSCs is trying to mimic natural processes, such as phothosynthesis, in order to obtain more clean and eco-compatible energy resources. However, despite the huge effort spent, the efficiency of solar cells based on natural dyes is still at least one order of magnitude lower than the ones based on Ru-dyes or perovskites. Some crucial features - especially the properties of the oxide/dye interface - are largely not explained and not-controlled in the wet-chemistry setups, usually adopted in DSSC realization. Some specific investigations of the interface at the atomic level are thus required.

From the theoretical side, a profitable strategy to get insight into this complex issue is to simplify the system and decouple the interaction processes, designing prototype models (e.g. molecule/oxide oxide/conductor, molecule/electrolyte interfaces), which include the correct interactions step-by-step in a controlled way. Here, we focus in particular on the metal-oxide interfaces with natural molecular dyes. The material of choice is the zinc-oxide that is a direct band-gap semiconductor crystallizing in the wurtzite structure and exhibiting high electron and thermal conductivity, efficient luminescence and strong excitonic effects even at room temperature. Due to its large gap (3.4 eV) ZnO is transparent and represents an attractive choice for applications in ultraviolet light emitters, field-effect transistors, sensors, piezoelectric devices and polariton laser. Due to its polar wurtzite structure,

ZnO may be easily grown in ordered array of nanostructures such as wires [5] and tetrapods, that have been profitably applied in DSSCs [8].

In the spirit of realizing "eco-green" cells, we consider as sensitizers a class of molecular dyes, namely anthocyanins [9], that mimic the light harvesting of natural systems. Along with chlorophylls and carotenoids, anthocyanins are the main natural pigments (from red to blue) in plants, flowers and fruits, i.e. they efficiently absorb visible radiation [10, 11]. Anthocyanins are natural molecules (belonging to flavonoids), constituted of three conjugated carbon-based rings, stabilized by a glucose sugar. Anthocyanins possess a catechol terminal group, proposed as active chromophore in optopelectronic systems [12, 13], and several OH hydroxyl terminations, useful for anchoring on surfaces. In solution, the electronic and optical properties of the molecule (i.e. the optical gap, and the absorption spectra) may be modulated in a controlled way as a function of pH [14]. From the analysis of the pigmentation of vegetables also follows that anthocyanins are able to chelate metallic ions (e.g. Al, Zn) and self-assemble in ordered stacked configuration, realizing a huge variety of structures with different colors (i.e. different optical properties) [15]. Previous ab initio investigations on a selected anthocyanins in gas phase [22, 23] and water solution [24–26] confirm both the thermodynamic stability of the molecule and its electro-optical changes at different pH configurations.

Because of their natural capability in adsorbing light over a large frequency spectrum and their high stability against photodegradation, anthocyanins (expecially cyanidin-3-glucoside aka cyanin) have been tested as dye in DSSCs, using both TiO_2 and ZnO as semiconducting mesoporous [16–21]. Despite a very intense sensitization of the metal-oxide system, the total efficiencies of the overall cells resulted to be ridiculously small ($< 0.5\%$). Many issues may contribute to this low yield, for instance (i) light adsorption and charge generation, (ii) charge recombination and (iii) energy barriers and charge transport. Here we investigate properties of cyanin/ZnO assembly, focusing on the band alignment resulting from the formation of the interface and its effects on both electronic and optical properties of the system.

2 Method

We performed first principles total-energy-and-forces simulations by using the code PWscf, included in the QUANTUM ESPRESSO suite [27]. The electronic structure is described by the density functional theory (DFT) within the PBE [28] generalized gradient approximation to the exchange-correlation functional. Single particle wavefunctions (charges) are expanded

on a plane-wave basis set up to a kinetic energy cutoff of 28 Ry (280 Ry). Ionic potentials are described by ab initio ultrasoft pseudopotentials of the Vanderbilt's type [29]; *3d*-shell of Zn metal is explicitly included as valence electrons. A regular (4×4) grid of **k**-points is used to sample 2D Brillouin zone of the interfaces.

The DFT description of ZnO bulk band structure provides a severe underestimation of the bandgap (E_g^{DFT}=0.7eV vs E_g^{exp}=3.3eV), well beyond the standard gap reduction given by DFT [30]. One possible and computationally inexpensive way to correct this behavior is to include an *ad hoc* Hubbard potential within the DFT+U scheme, as initially proposed by Janotti and coworkers [31]. Here, we included an Hubbard potential U=12.0 eV on the *3d* orbitals of zinc and U=6.5 eV on the *2p* orbitals of oxygen. These specific values of U parameters result from a fine fit that reproduces the experimental ZnO bulk band structure [30]. This procedure has been adopted by many authors, providing very similar values for the used U parameters as well as very similar corrections to the electronic structure. [32–34] A detailed set of accuracy tests on the effect of DFT+U (same set of parameters) on the electronic structure of both ZnO bulk and surfaces can be found in Refs [35].

The interface is simulated using periodically repeated supercells. The unit cell has a (2×3) lateral periodicity and contains six bilayers of ZnO wurtzite semiconductor exposing the non-polar $(10\bar{1}0)$ surface. One cyanidin molecule is symmetrically adsorbed on each surface. Slab replicas are separated by ∼12 Å of vacuum (see Figure 1). The lattice parameters of the surfaces are obtained from the optimization of the corresponding bulk crystal. Each structure is optimized until forces on single atoms are smaller than 0.03 eV/Å.

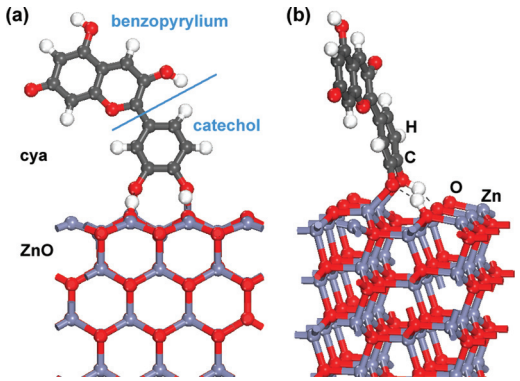

Figure 1 Front (a) and side (b) view of cyanidin/ZnO$(10\bar{1}0)$ interface. Blue line identifies the catechol and benzopyrylium subunits of cyanidin molecule.

The absorption spectra are calculated in the independent particle approximation from the complex dielectric function, evaluated using the code epsilon.x, also included in the QUANTUM ESPRESSO suite, which implements a band-to-band formulation of the Drude-Lorentz model for solids [36, 37]. The simulation of the color is obtained following the *tristimulus* colorimetry theory [38], which provides the red (R), green (G), and blue (B) representation of the perceived hue, starting from the knowledge of an illuminant source (solar light D65) [39], the retina matching functions (tabulated) [39] and the absorption spectrum (calculated) [22, 25, 26].

3 Results and Discussion

In natural systems, anthocyanins are stabilized by one or more sugar units, usually bonded to the benzopyrylium unit. Despite this stabilization role, it has been demonstrated that sugars do not play a direct role either in the adsorption onto a semiconductor surfaces, or in the optical properties of the dye. Indeed, the adsorption on metal oxide surfaces is realized through the chelating catechol group (see Figure 1a), which easily forms dative bonds with the outermost exposed metal atoms. On the other hand, the lowest energy optical transitions, which characterize the color activity in the visible range, have a typical $\pi \rightarrow \pi^*$ behavior, associated to π-like conjugated single particle orbitals distributed only on the benzopyrylium and catechol subunits, but not on the sugar unit [22, 25]. The latter contributes to optical spectrum only at higher energies in the UV range. For these reasons, we here consider only the adsorption of the aglycone form of cyanin, also known as cyanidin (cya).

In particular, we considered the adsorption of cyanidin on the non-polar surfaces of ZnO, and we compared the results with the paradigmatic case of catechol/ZnO interface for completeness [35]. The optimized clean $(10\bar{1}0)$ surface exhibits a strong reorganization of the outermost layer, which relaxes forming ordered rows of tilted dimers along the $[1\bar{2}10]$ direction (see Figure 1).

We prepared the starting configuration setting the molecule at $\sim$3.2 Å from the surface, with the catechol ring perpendicular to the exposed dimers. After the relaxation process, cya remains almost perpendicular to the surface (see Figure 1) with both the oxygen atoms of the catechol units bonded do two consecutive Zn atoms of substrate. During the relaxation path, the two –OH terminations of catechol point toward two next-neighbor dimers of the surface, and release one H^+ proton that is promptly captured by frontal oxygen atom, making a O-H bond. In the final configuration, the molecule is partially deprotonated and forms two chemical Zn-O and two hydrogen O-H-O bonds

with the surface. This corresponds to charge transition of the molecule from the positively charged *flavylium* phase to the neutral *quinonoidal* one, in agreement with experimental results [16]

The electronic structure of the resulting interface is summarized in Figure 2 that shows the total (black line) and projected density of states (DOS) on ZnO substrate (shaded area) and cyanidin (blue line) contributions. Similar to the case of the catechol adsorption [35], cya only slightly perturbs the valence band top (VBT) and the conduction band minimum (CBM) of the surface that remains similar to the clean surface case [35]. Zn-O binding orbitals are detected at lower energy (ca. –2.0 eV) in the valence band and result from a charge transfer from Zn dimer atoms to catechol oxygens.

The gap area (see inset of Figure 2) is dominated by the presence of a set of occupied molecular states, including in particular the HOMO (H_m) orbital of the original cyanidin. All these gap states have a π character with contributions on both the catechol and the benzopyrylium rings, in agreement with previous theoretical investigations [22, 23]. The overlap with surface states is negligible. The corresponding LUMO state (L_m) of the dye is set at higher energy ($\sim$4.2 eV) in the conduction band. It also has a π character

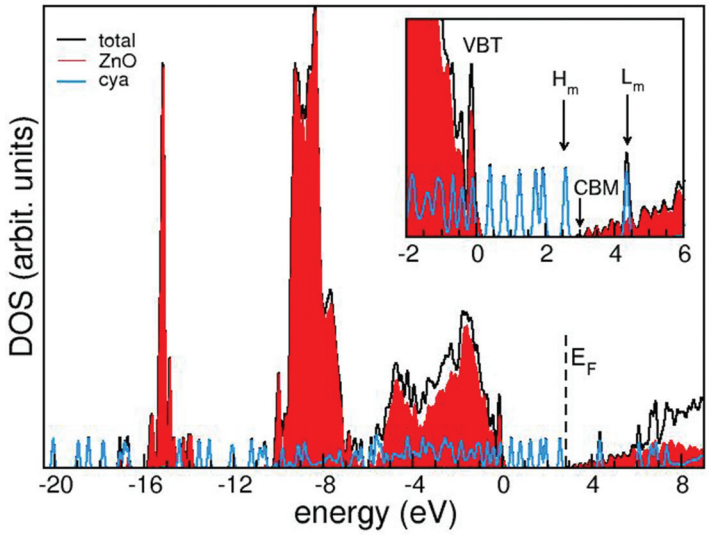

Figure 2 Total DOS (black line) and projected contributions on ZnO substrate (shaded area) and cyanidin (blue line) for the molecule/surface interface. The zero of the energy scale is aligned to the top of the valence band of the clean ZnO surface. Vertical dashed line identifies the Fermi energy for the interface. Inset zooms over a region around the band gap.

and it is partially overlapped with the ZnO electronic states at the surface. The resulting effective gap of the interface (CBM-H_m) is reduced to 0.5 eV and corresponds to the formation of a type-II staggered interface, which is the desired prerequisite for the realization of excitonic solar cells, such as DSSCs.

In order to confirm the sensitization effect of cya on ZnO surface, we calculated the single particle absorption spectra for the overall interface that we compare with spectra of its separate constituents. The results are shown in Figure 3, along with the simulation of the corresponding perceived colors. Although underestimated by DFT approaches (no gap corrections are included for the molecule), cya exhibits lowest energy absorption peaks in the visible range, confirming is color dye activity in natural systems. On the contrary, clean surface has its absorption edge in the UV range ($\sim$3.3 eV), resulting transparent in the visible range, as confirmed by the simulated color shown in the inset of Figure 3. Once the interface is formed, we identify contributions to absorption spectrum from both the VBT $\rightarrow$ CBM of ZnO surface and (rather slightly blue-shifted) the $H_m \rightarrow L_m$ molecular transitions. Further, a new sub-bandgap absorption peak appears at $\sim$1.7eV, corresponding to a *direct* cya $\rightarrow$ ZnO transitions. As a consequence of this absorption activity in the visible range, the substrate is no more transparent as shown in Figure 3, in agreement with the experimental results [16, 18, 21].

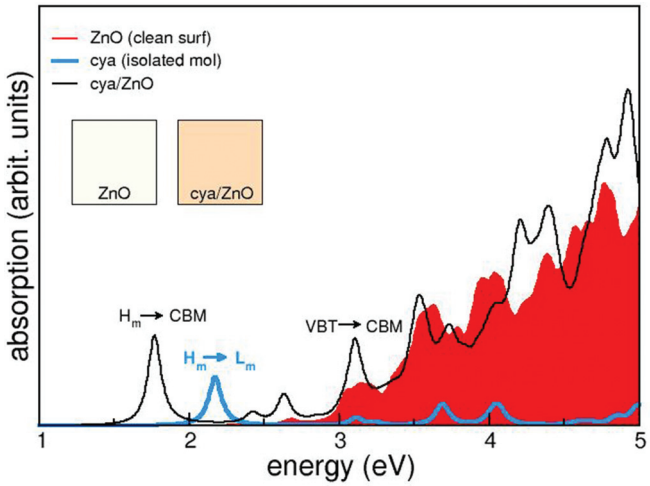

Figure 3 Absorption spectra for clean ZnO surface (shaded area), isolated cya molecule (blue line) and cya/ZnO interface (black line). Insets show the simulated perceived colors corresponding to the bare (left) and functionalized (right) surface.

This specific band alignment and the consequent absorption spectrum have important effects in the working processes of the corresponding solar cells: (1) the inclusion of cya actually sensitizes the substrates allowing for light harvesting in the near-IR-visible range, which is positive for the realization of DSSCs. (2) The existence of direct molecule-to-surface optical transitions and the proximity of the molecular H_m state to the CBM of ZnO are detrimental for the efficiency of the final device.

In standard DSSCs, excitons form in the dye and the photo-excited electrons are injected into the conduction band of the metal oxide through the excited LUMO of the dye. Since the molecular LUMO is higher in energy with respect to the CMB (type-II interface), the back-donation to the starting molecular state is prohibited. The LUMO-mediated charge injection, also associated to non-radiative phonon interactions, is a relatively slow process (hundreds of fs), which allows for the reduction of the hole in the molecule by the electrolyte. This strongly reduces the radiative electron-hole recombination process and gives rise to an effective photocurrent. In the present case, instead, if the direct cya-to-ZnO transitions assure an ultrafast photocharge injection into the semiconductor, the absence of any energy barrier favors the charge recombination with the left hole remained on the molecular site and not yet regenerated by the electrolyte.

In addition, the proximity of cya HOMO to the CBM of ZnO causes a dramatic reduction of the effective open-circuit potential (V_{OC}) for the device. The open-circuit potential is defined as the difference between the Fermi level of the electrode attached to the metal-oxide and the reduction-potential of the electrolyte. The Fermi level of standard metal electrodes (e.g. Cu, Au) are very close to the conduction band of ZnO. If the reduction potential lyes in the gap region but at an energy level lower than molecular HOMO, the formal V_{OC} could be reasonably high. Unfortunately, in this case the electrolyte would not be able to regenerate the hole charge in the molecule. This would interrupt the light harvesting process and the consequent photo-current generation. Thus, in order to regeneration process take place, it is necessary that the reduction potential of the electrolyte lyes between the CBM of the metal-oxide (i.e. of the Fermi level of the counter electrode) and the HOMO of the molecule. However, due to small effective CBM-H_m gap, the resulting V_{OC} potential is therefore very small.

We can conclude that despite the favorable sensitization action, the formation of cya/ZnO interface is plagued by high charge recombination processes and very low V_{OC} potential, or alternatively very low photo-current generation. In both cases this corresponds to a very low generated

power, i.e. to very low efficiency of the resulting solar cells. This explains the unsatisfying results collected in the experimental measurements, in the presence of anthocyanin sensitizers.

Notably, these results are qualitatively not affect by the choice of the exchange-correlation functional used in the simulation: the use of hybrid functionals such as B3LYP or PBE0 impart a slight downshift of the ionization potential of the molecule by –0.53 eV and –0.73 eV and an upshift of the electron affinity by +0.48 eV and +0.84 eV, respectively. This does not change, however, either the symmetry of the molecular orbitals or the order alignment with respect to the gap states of the ZnO and thus the picture described above.

4 Conclusions

We carried out ab initio simulations of the cyanidin/ZnO interface, as prototype of the anthocyanin/metal-oxide active elements, experimentally proposed as metal-free and "green" DSSCs. The resulting electronic structure realizes the type-II band-alignment requested in excitonic solar cells, while it is detrimental for the charge separation and establishment of a net open-circuit potential. Thus, our results well explain both the positive sensitization process due to cyanidin and the low conversion efficiency reported in the experiments. This suggests that, even though suitable for educational class experiments, anthocyanins are not a valuable choice for the actual realization of high performance solar cells.

Acknowledgments

AC kindly thanks Alice Ruini, Alessandra Catellani and Stefano Baroni for help and discussions. This work has been founded in part by MIUR through project PREMIALE EoS.

References

[1] *Nanostructured Materials for Solar Energy Conversion*. Edited by T. Soga Elsevier, (2006).

[2] B. O'Regan and M. Gratzel. A low-cost, high efficiency solar cell based on dye-sensitized colloidal TiO−2 films. *Nature*, **353**:737–740, (1991).

[3] M. K. Nazeeruddin, S. M. Zakeeruddin, J.-J. Lagref, P. Liska, P. Comte, C. Barolo, G. Viscardi, K. Schenk, and M. Gratzel. Stepwise assembly of amphiphilic ruthenium sensitizers and their applications in dye-sensitized solar cell. *Coord. Chem. Rev.*, **248**:1317–1328, (2004).

[4] J.-J. Cid, J.-H. Yum, S.-R. Jang, M. K. Nazeeruddin, E. Martinez-Ferrero, E. Palomares, J. Ko, M. Gratzel, and T. Torres. Molecular Cosensitization for Efficient Panchromatic Dye-Sensitized Solar Cells. *Angew. Chem. Int. Ed.*, **46**:8358–8362, (2007).

[5] M. Law, L. E. Greene, J. C. Johnson, R. SAaykally, and P. Yang. Nanowire dye-sensitized solar cells. *Nature Mater.*, **4**:455–459, (2005).

[6] J.-Y. Liao, B.-X. Lei, H.-Y. Chen, D.-B. Kuang, and C.-Y. Su. Oriented hierarchical single crystalline anatase TiO2 nanowire arrays on Ti-foil substrate for efficient flexible dye-sensitized solar cells. *Energy & Environ. Sci.*, **5**:5750–5757, (2012).

[7] H.-J. Snaith and L. Schmidt-Mende. Advances in Liquid-Electrolyte and Solid-State Dye-Sensitized Solar Cells. *Adv. Mater.*, **19**:31873200, (2007).

[8] J. A. Anta, E. Guillen, and R. Tena-Zaera. ZnO-Based Dye-Sensitized Solar Cells. *J. Phys. Chem. C*, **116**:11413–11425, (2012).

[9] *Anthocyanins, Biosynthesis, Functions and Applications*. K. Gould, K. Davies, C. Winefield, Eds.; Springer Science+Business Media LLC: New York, (2009).

[10] R. L. Jackman, R. Y. Yada, M. A. Tung, and R. A. Speers. Anthocyanins as Food Colorants: a Review. *J. Food Biochem.*, **11**:201–247, (1987).

[11] F. J. Francis and P. C. Markakis. Food Colorants: Anthocyanins. *Crit. Rev. Food Sci. Nutr.*, **28**:273–314, (1989).

[12] R. Brouillard. Flavonoids and flower colour in *The Flavoids* Ed. By J.B. Harborne, (Chapman and Hall), (1988).

[13] L. Rustioni, F. Di Meo, M. Guillaume, O. Failla, and P. Trouillas. Tuning Color Variation in Grape Anthocyanins at the Molecular Scale. *Food Chem.* **141**:4349–4357, (2013).

[14] B. Gordillo, F. J. Rodriguez-Pulido, M. E. M. Gonzalez-Miret, and F. J. Heredia. Comprehensive Colorimetric Study of Anthocyanic Copigmentation in Model Solutions. Effects of pH and Molar Ratio. *J. Agric. Food Chem.*, **60**:2896–2905, (2013).

[15] T. Goto and T. Kondo. Structure and Molecular Stacking of Anthocyanins Flower Color Variation. *Angew. Chem. Int. Ed.*, **30**:17–33, (1991).

[16] N J. Cherepy, G. P. Smestad, M. Gratzel, and J. Z. Zhang. Ultrafast Electron Injection: Implications for a Photoelectrochemical Cell Utilizing an Anthocyanin Dye-Sensitized TiO2 Nanocrystalline Electrode. *J. Phys. Chem. B*, **101**:9342–9351, (1997).

[17] P.M. Sirimanne, M.K.I. Senevirathna, E.V.A. Premalal, P.K.D.D.P. Pitigala, V.Sivakumar, and K. Tennakone. Utilization of natural pigment extracted from pomegranate fruits as sensitizer in solid-state solar cells. *J. Photochem. Photobiol. A: Chem.*, **177**: 324327, (2006).

[18] S. Hao, J. Wu, Y. Huang, and J. Lin. Natural dyes as photosensitizers for dye-sensitized solar cell. *Solar Energy*, **80**:209–214, (2006).

[19] G. Calogero and G. Di Marco. Red Sicilian orange and purple eggplant fruits as natural sensitizers for dye-sensitized solar cells. *Sol. Energ. Mat. Sol.*, **92**:1341–1346, (2008).

[20] K. Wongcharee, V. Meeyoo, S. Chavadej. Red Sicilian orange and purple eggplant fruits as natural sensitizers for dye-sensitized solar cells. *Sol. Energ. Mat. Sol.*, **91**: 566–571, (2007).

[21] D. Zhang, N. Yamamoto, T. Yoshida, and H. Minoura. Natural dye sensitized solar cells. *Trans. Mater. Res. Soc. Jpn.*, **27**:811–814, (2002).

[22] X. Ge, A. Calzolari, and S. Baroni. Optical properties of anthocyanins in the gas phase. *Chem. Phys. Lett.* **618**:24–29, (2015).

[23] A. Calzolari, D. Varsano, A. Ruini, A. Catellani, R. Tel-Vered, H.B. Yildiz, O. Ovits, and I. Willner. Optoelectronic properties of natural cyanin dyes. *J. Phys. Chem. A* **113**: 8801–8810, (2009).

[24] A. Calzolari, S. Monti, A. Ruini, and Alessandra Catellani. Hydration of cyanin dyes. *J. Chem. Phys.*, **132**:114304, (2010).

[25] O.B. Malcioglu, A. Calzolari, R. Gebauer, D. Varsano and S. Baroni. Solvation and thermal effects on the optical properties of natural dyes: a case study on the flavylium cyanin. *J. Am. Chem. Soc.*, **133**:15425–15433, (2011).

[26] X. Ge, I. Timrov, S. Binnie, A. Biancardi, A. Calzolari, and S. Baroni. Accurate and inexpensive prediction of the color optical properties of anthocyanins in solution. *J. Phys. Chem. A*, **119**:3816–3822, (2015).

[27] P. Giannozzi, et al. QUANTUM ESPRESSO: a modular and open-source software project for quantum simulations of materials. *J. Phys.: Condens. Matter*, **21**:395502 (2009). See also www.quantum-espresso.org.

[28] J. P. Perdew, K. Burke, and M. Ernzerhof. *Phys. Rev. Lett.*, **77**:3865–3868, (1996).

[29] D. Vanderbilt. Soft self-consistent pseudopotentials in a generalized eigenvalue formalism. *Phys. Rev. B*, **41**:R7892–R7895, (1990).

[30] D. Vogel, P. Krüger, J. Pollmann. Self-interaction and relaxation-corrected pseudopotentials for II–VI semiconductors. *Phys. Rev. B*, **54**:5495–5511, (1996).

[31] A. Janotti and C. G. Van de Walle. Native point defects in ZnO. *Phys. Rev. B*, **76**: 165202, (2007).

[32] Y. Dong and L. J. Brillson. First-Principles Studies of Metal (111)/ZnO(0001) Interfaces. *J. El. Mater.*, **37**:743–748, (2008).

[33] X. Ma, Y. Wu, Y. Lv, and Y. Zhu. Correlation Effects on Lattice Relaxation and Electronic Structure of ZnO within the GGA+U Formalism. *J. Phys. Chem. C*, **117**: 26029–26039, (2013).

[34] L. A. Agapito, S. Curtarolo, and M. Buongiorno Nardelli. Reformulation of DFT+U as a pseudo-hybrid Hubbard density functional. *Phys. Rev. X*, **5**:011006, (2015).

[35] A. Calzolari, A. Ruini, and A. Catellani. A. Anchor group versus conjugation: towards the gap- state engineering of functionalized ZnO(10-10) surface for optoelectronic applications. *J. Am. Chem. Soc.*, **133**:5893–5899, (2011).

[36] A. Calzolari, A. Ruini, and A. Catellani. Transparent Conductive Oxides as Near-IR Plasmonic Materials: The Case of Al-Doped ZnO Derivatives. *ACS Photonics*, **1**: 259–261, (2014).

[37] R. Colle, P. Parruccini, A. Benassi, and C. Cavazzoni. Optical properties of emeraldine salt polymers from ab initio calculations: comparison with recent experimental data. *J. Phys. Chem. B*, **111**:2800–2805, (2007).

[38] N. Ohtha, A. R. Robertson. Colorimetry: Fundamentals and applications, John Wiley & Sons Ltd UK (2005).

[39] http://en.wikipedia.org/wiki/CIE$_1$931_color_space.

Biography

A. Calzolari. AC graduated in physics in 2003 at University of Modena and Reggio Emilia in Modena, Italy. He is researcher at the Instituto Nanoscienze of the National Research Council of Italy (CNR-NANO) since 2010. He is also adjunct professor at Physics Dept., University of North Texas, Denton TX, USA since 2012; and Member of Aflowlib Consortium, Duraham NC USA since 2015. His research activity is focused on the ab initio study of the structural, electronic, optical, vibrational and transport properties of nanostructures, molecules, surfaces and interfaces, for solar cells, molecular electronics and nanotechnology applications.